Analytical Methods

Accepted Manuscript

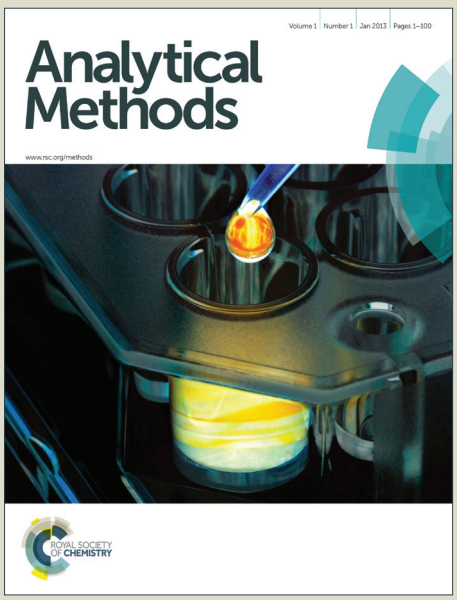

ROYAL SOCIETY OF CHEMISTRY

www.rsc.org/methods

Analyst

ARTICLE

Lab on Phone citrate capped silver nanosensor for lidocaine hydrochloride detection from biological matrix

Received 00th January 20xx,
Accepted 00th January 20xx

DOI: 10.1039/x0xx00000x

www.rsc.org/

Niha Ansari,[a] Anand Lodha,[a] Alok Pandya,[b] Pinkesh Sutariya[c], S. K. Menon[*a]

In present investigation, we applied the application potentiality of nanomaterials and smartphone analysis to develop the specific, sensitive and portable method. In this study, we report a silver nanoparticles based colorimetric nano sensor for determination of lidocaine hydrochloride (LHC) up to 0.05 ng/ml with good linear correlation in the range from 0.1 to 4.5 ng/ml with a correlation coefficient of 0.9914. Coexisting substances including acetaminophen, diazepam, nitrazepam, lorazepam, ambien, atropine and bupivacaine did not interfere in the determination of LHC. The developed sensor proved to be a smart alternative and lab on phone device which would help in on spot determination of LHC in forensic toxicological drug screening. Here we utilized easily accessible vitreous humor which is often unnoticed for toxicological drug screening along with blood for real sample analysis.

Introduction

In present state, there are few analytical methods for psychotropic substances in biological samples, and the great majority of intoxications were reported on the mere basis of anamnestic and clinical data that often suffer from low sensitivity, specificity and tedious lengthy procedures requiring bulky and expensive sophisticated instrumentation[1]. Individually, every biological matrices possesses its own idiosyncrasies along with the pros and cons of usage. For any forensic toxicological analysis, it is important to have proper acquaintance of analytes stability in biological matrix as if once variations arise in the time interval between collection, transportation and analysis it will prolong and give inaccurate results[2]. Traditionally, blood, urine and viscera are used for forensic toxicological analysis. Another post-mortem fluid which is often unnoticed is vitreous humor which is easily accessible. As compared to blood and urine, vitreous humor is well protected and has a liquid eccentric. Vitreous resists putrefaction, less subjected to contamination and post-mortem biochemical changes ensue leisurely in eye[3]. Moreover, in cases involving trauma to central organs, vitreous humor is the only matrix which remains uncontaminated as blood also get contaminated due to tissues and stomach contents. Even in cases of severely burned, embalmed or bleeding-shocked bodies vitreous is well protected and can be used for post-mortem analysis. This makes vitreous an important biological matrix for analysis purpose. Vitreous humor consists of 99% water and has viscosity approximately two times that of water[4]. In analytical relations, as compared to blood or its derivatives (serum and plasma) and urine, vitreous has a relatively simple matrix which has been recommended for several xenobiotics analysis of forensic interest[2, 5 - 7]. Generally, vitreous is used for the analysis of alcohol and glucose levels during post-mortem toxicological analysis. Now a day it is also being progressively used for detection of drugs to determine possible cause of death. Number of papers have discussed vitreous drugs analysis by using target drug analysis approach, such as antidepressants, barbiturates, cocaine and its metabolites[8–11], methadone, meprobamate, amphetamines[12, 13], benzodiazepines[14, 15], opiates[11], LSD and metabolites[16], cannabinoids[17] and morphine are studied till now[18]. It has also been found that tyramine and phenethylamine interfere in drug extraction from blood and tissue specimens while these factor is less the in case of vitreous humor drug analysis[4]. Vitreous applicability for the analysis of immunological drugs of abuse has also been studied. Vitreous humor is considered to be better alternative in cases where urine is not available as vitreous humor is closer to blood than urine and all the analytes which are carried by blood through active and passive transport through the blood-retinal barrier get absorbed in VH[19].

Lidocaine is an aromatic amide which is widely used as local anesthetics[20]. It is used in topical anesthesia, intradermal infiltration, and peripheral nerve blocks[21]. It is used topically to relieve itching, burning and pain from skin inflammations, injected as a dental anesthetic, and in minor surgery[22]. Lidocaine hydrochloride inhibits voltage-gated sodium channels and affects potassium channels, GABAA receptors and NMDA receptors[21]. Normal level of lidocaine to get effective in serum is l-6 pg/ml and its metabolites produces

[a] Department of Forensic Science, School of Sciences, Gujarat University, Ahmedabad, Gujarat-380009, India. E-mail: shobhanamenon07@gmail.com; n.ansari3@gmail.com; forensicwithanand@gmail.com
[b] Department of Chemistry, School of Sciences, Gujarat University, Ahmedabad, Gujarat-380009, India.
[c] Bhavans Shree I. L. Pandya Arts, Science College, Dakor 388225, Gujarat, India.
Electronic Supplementary Information (ESI) available: See DOI: 10.1039/x0xx00000x

toxicity in body at high concentrations when it is greater than 6 pg/ml[20]. Cases are reported where accidental fatalities and suicides following intravenous injection of lidocaine, medical homicide and extreme negligence in epidural anesthesia occurring as well as death due to high spinal anesthesia[22, 23]. Cases are also reported where lidocaine is found to be associated with cocaine in drug users[22]. Increase in number of such cases therefore levies to develop a technique which is simple, fast and sensitive for the determination of lidocaine in biological matrices. At present lidocaine is frequently determined by the use of gas chromatography (GC) with flame ionization, nitrogen and phosphorous detector (NPD), or mass spectrometry (MS)[24-28]. The use of such sophisticated instruments is not convenient for on spot, rapid detection of lidocaine as the use of such instruments require tedious sample preparation involving the use of toxic solvents. These problems can be overcome by the use of nanomaterials. Nanotechnology is showing rapid increase in relation to size-related physico-chemical properties[29]. Recently, metal nanoparticles-based UV–visible spectrometric methods have gained much attention for selective and sensitive detection of targeted analytes in various complex matrices. Metal nanoparticles have shown their application in various fields, including catalysis, sensing, photochemistry, optoelectronics, energy conversion and medicine[30]. Now a day's metal nanoparticles are used as capable coloring probes for selective, on-site and real-time colorimetric sensing with naked eye detection. In recent years silver nanoparticles has gained much attention of researchers due to their unique physical, chemical and biological properties. Silver nanoparticles (AgNPs) have distinguishing physico-chemical properties such as high electrical and thermal conductivity, surface-enhanced Raman scattering, chemical stability, catalytic activity and nonlinear optical behavior[31]. AgNPs are considered to be less toxic and biocompatible due to which they are extensively explored for various biological applications. Silver nanoparticles functionalized with various organic derivatives such as *p*-sulfonatocalix[4]arene, oligonucleotide, *p*-nitroaniline dithiocarbamate, and 4,4-bipyridine are applied for colorimetric sensing of various organic molecules such as pesticides, amino acids and DNA, however no endeavors are made for the detection of lidocaine by use of unmodified silver nanoparticles. Herein, we demonstrate the potential use of AgNPs as colorimetric sensor for simple, rapid, highly sensitive, cost effective and on spot detection of lidocaine hydrochloride from blood and vitreous humor.

Recently, for the first time our research group successfully applied the nanomaterials for forensic toxicological drug screening from skeletal remains targeting the investigation on cause of death[32, 33]. Further we utilized the smartphone to provide the portability and cost effectiveness to the developed colorimetric sensor. Smartphone based colorimetric detection is an innovative technology which have attracted various authors to utilize smartphone as colorimetric sensor[34-36]. Smartphone have gained popularity due to the presence of built-in camera with high resolution. Smartphone provide a simple colorimetric detection, especially when naked eye alone is not sufficient, and prove to be good substitute to a scanner[37]. The colorimetric data procured form smartphone as a digital image can be further converted to analytes concentrations. This advancement in technology provides a new direction in colorimetric detection by replacing unwieldy spectrophotometers. In the present study, we introduce a simple approach for colorimetric detection of lidocaine hydrochloride from vitreous humor based on the calculation of the RGB values (Red, Green and Blue color) of the digital images using Adobe Photoshop CS6 and smartphone app, taken from iPhone 5S under optimized conditions in safety cabinet. To check the robustness of the developed smartphone based colorimetric nano probe other instrumental techniques were employed.

Methods and materials

All the chemicals used in the present work are of highest purity. All the solutions were prepared in Milli Q water having resistivity 18 Ω. All the chemicals namely silver nitrate, tri sodium citrate and sodium dodecyl sulphate (SDS) were purchased from Sigma Aldrich. The characterization of the synthesized particles was done by using UV-Vis spectrophotometer, FTIR (Fourier transform infrared spectrometer), and Dynamic Light Scattering (DLS). UV-Vis absorption spectra were obtained on a Shimadzu 1800 UV-Vis spectrophotometer, IR spectra were measured with a Bruker Tensor-32 FT-IR spectrometer, Transmission electron micrographs (TEM) were recorded on JEOL, JEM-2100 (200 kV) and DLS measurements were performed using Metrohm Nanotrac instrument.

Synthesis of unmodified silver nanoparticles

Silver colloidal solution was prepared in modified CEM Discover Benchmate microwave using single mode and continuous power at 2.45 GHz by the reduction of $AgNO_3$ using tri-sodium citrate by our reported method with minor modifications[38]. All glassware prior to the synthesis were carefully cleaned with freshly prepared 3:1 HCl/HNO_3 (aqua regia) and rinsed with Milli-Q water. The synthesis process of silver nanoparticle was carried out in a microwave at single mode having a continuous power at 400 W. The whole synthesis process of silver nanoparticle was carried out in reaction flask containing 20 mL of 2 mM $AgNO_3$ solution, 10 % 10 µl SDS and 100 µL of 18 mM tri sodium citrate which was heated at 400 W for 20 sec. The solution changed from colourless to yellow to yield Ag nanoparticles of 36 nm. A sharper surface plasmon resonance (SPR) band at 420 nm observed for the citrated capped AgNPs ensured the formation of homogeneously dispersed, uniformly shaped and relatively smaller nanoparticles. SDS was added to increase the stability of the particle for longer duration.

Detection of Lidocaine using unmodified AgNPs as a probe

For each measurement, 0.5 ml of lidocaine hydrochloride (LHC) solution of 1-10 ng/ml was added in to the 1.5 ml colloidal solution of 2 mM AgNPs and 2 ml of 7 pH PBS into a 5 ml test tube and reaction mixture was mixed and allowed to stand for 30 sec at room temperature (25°C). The yellow solution of AgNPs turns to red color upon the addition of lidocaine and this colorimetric change was clearly visible by the naked eye. The absorption spectra of the resulting solutions were recorded at 506 nm with UV-Vis spectrophotometer, Shimadzu 1800. Further, the resulting solution was transferred to 2 ml Eppendorf tube and photographs were recorded using iPhone 5S under optimized conditions for image analysis. The DLS and FTIR analysis were done to measure the hydrodynamic diameter and morphological changes induced by lidocaine in silver nanoparticles.

Smart phone analysis

For smart phone analysis a polystyrene foam box was prepared as shown in **Fig. S1**, **see ESI**. All the sides of the box were covered with white plain paper sheet to get similar environment and light conditions. The dimension of the box outside was 20 x 25 x 20 cm (width x length x height) and inside was 10 x 10 x 10 cm. On the top of the box a LED light was attached to get good amount of light while procuring images by placing the mobile phone iPhone 5S at the centre position of the box as shown in **Fig. S1**, **see ESI**. The Eppendorf tube was placed at a fixed point and all the images were taken in the similar manner. All the photographs were taken by iPhone 5S in a "flash-off" mode to obtain similar lighting condition and surrounding environment. In order to facilitate more incident light to reach the light-sensing silicon iPhone 5S's backside illumination CMOS image sensor was used which allows the light to strike the photocathode layer without the interference of backside illumination CMOS sensor. This property allows detecting small differences in photon emission. Every photograph digital image was saved as a Joint Photographic Experts Group (JPEG) format (24 bit) on the iPhone's memory which was later transferred to computer and processed in Adobe Photoshop CS6. The intensity of the red, green and blue colors was measured by placing a box of size 100x100 pixels on each Eppendorf vials. The average of the red, green and blue colors intensity was recorded in an Excel spreadsheet and calibration curves of concentration against the intensity of the red, blue, green and total RGB was obtained. In the present study we also utilized the software Colorhelper obtained from app store. All the images were processed in the software to determine the RGB values by placing the circle having radius 1 cm, which is self-automated feature of the app. All the intensities were recorded in an Excel spreadsheet and calibration curves of concentration against the intensity of the red, blue, green and total RGB was obtained. The schematic representation of the process is shown in **Fig. 1**.

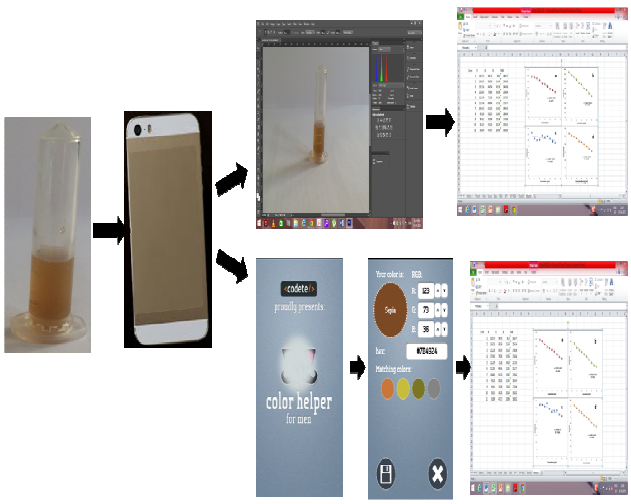

Figure 1 Schematic illustration of resultant color products via Adobe Photoshop and ColorHelper application

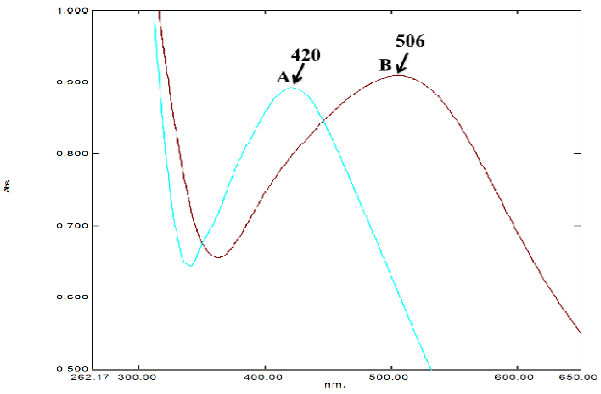

Figure 2 Showing UV-Vis spectra of silver nanoparticle after the addition of lidocaine

Results and Discussion

UV-Vis Spectrophotometry

UV-Vis absorption spectrometry was used to explore the change in the AgNPs induced by LHC. As shown in **Fig. 2**, the AgNPs showed a surface plasmon resonance peak at 420 nm and upon the addition of lidocaine, a peak at 506 nm upturns resulting in a red shift. A new and strong absorbance peak appeared at 506 nm, owing to the aggregation of AgNPs. Meanwhile, the colour of the resulting suspension of the AgNPs clearly changed from yellow to red, indicating the aggregation of the AgNPs. It was found that as the concentration of lidocaine increases the intensity of the peak at 506 nm also increases, as a result of increased consumption of AgNPs which further leads to more and more aggregation. This observation confirms the decrease in the inter-particle distance of unmodified AgNPs, which results in change in color from yellow to red and shows a significant red-shift in the plasmon band energy to longer wavelength.

In addition, the sensitivity of the AgNPs was evaluated by varying the concentration of analyte LHC and the corresponding UV-Vis absorption spectra are shown in **Fig. S2**, **see ESI**. It is observed that the SPR band of citrate-capped AgNPs-LHC complex gradually increases with increasing

concentration of LHC from 0.1 to 4.5 ng/ml, yielding new SPR peaks at 506 nm from 420 nm SPR band of citrate capped-AgNPs. The correlation coefficient, of the linear range 0.1 to 4.5 ng/ml is 0.9914 from UV-Vis study as shown in **Fig. S3, see ESI**. The regression equation is y = 0.1273x + 0.0559, where (y) is the absorption ratio and (x) is the concentration of LHC in ng/ml.

Smart phone analysis results

The smartphone analysis was also performed to evaluate the minimum detectable concentration of LHC. The coloured product of AgNPs–LHC complex were analysed by using Colorhelper application and Adobe Photoshop CS6. The RGB values obtained in both the cases were in correlation with each other as both the results showed decrease in the intensity of red and green color as the concentration increases. In case of Colorhelper application, the linear equation for red color was y = -5.9152x + 144.73 and for green color was y = -5.4515x + 100.13 having excellent correlation coefficient R^2 = 0.9901 and R^2 = 0.991 respectively as shown in **Fig. 3**. While, in case of Adobe Photoshop CS6 the linear equation for red and green color was y = -6.1324x + 146.48 and y = -5.441x +

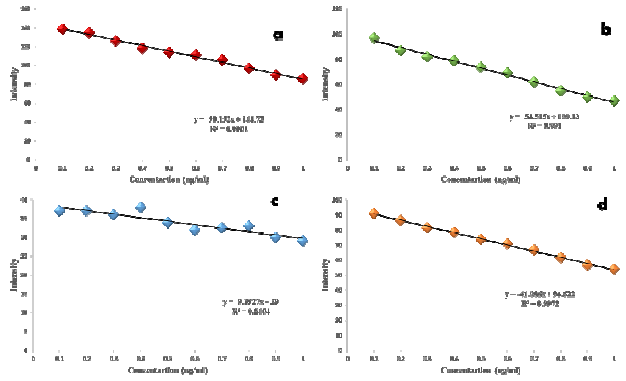

Figure 3 Relationship between (a) intensity of red light, (b) intensity of green light, (c) intensity of blue light, (d) intensity of total RGB and LHC concentration (0.125-1.25 ng/ml) from iPhone 5S images processed by Colorhelper app.

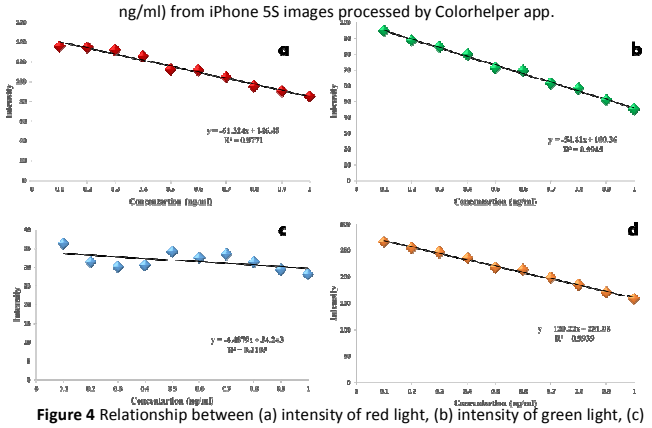

Figure 4 Relationship between (a) intensity of red light, (b) intensity of green light, (c) intensity of blue light, (d) intensity of total RGB and LHC concentration (0.125-1.25 ng/ml) from iPhone 5S images processed by Adobe Photoshop.

100.36, respectively with good correlation coefficient R^2 = 0.9771 and R^2 = 0.9945 as shown in **Fig. 4**. The result shows good relationship between the red and green colour intensity and LHC concentration ranging from 0.125-1.25 ng/ml, whereas the blue color intensity does not show any significant relation with LHC concentration. This results signify that the no any blue light is reflected from the color product where green and red colour are reflected from the colour product, LHC-AgNPs complex. The linear equation for total RGB in case of Colorhelper application was y = -4.1006x + 94.622 and in case of Adobe Photoshop CS6 was y = -12.022x + 281.08, respectively with excellent correlation coefficient R^2 = 0.9972 and R^2 = 0.9939. The results showed that the correlation coefficient for total RGB was more significant in case of app as compared to Adobe Photoshop CS6. The use of smartphone as image capturing device and transferring the image from mobile to computer software is time consuming whereas use of smartphone as image capturing device as well as for image processing using in build android application like Colorhelper not only save the time but also gives more significant results. Moreover, it gives portability for on spot recognition as well as quantification of LHC.

Dynamic light scattering measurements

To evaluate the aggregation of AgNPs-LHC we have employed a dynamic light scattering (DLS) technique. The results illustrated that silver nanoparticles have average hydrodynamic diameter of 36 nm as shown in **Fig. S4A**, **see ESI**. Addition of lidocaine to the silver nanoparticles resulted in aggregation and an increase in size to 420 nm as shown in **Fig. S4B**, **see ESI**. The DLS histogram clearly confirms the interaction between AgNPs and lidocaine. A change in the morphology of AgNPs in the presence of lidocaine indicates that the inter-particle distance of AgNPs decreases which strongly suggest that lidocaine induced aggregation of AgNPs. This allows us to develop a simple colorimetric sensing platform for the detection of lidocaine by UV-Visible spectrophotometer, which can be pragmatic visually with naked-eye.

TEM analysis

Further to evaluate the aggregation of AgNPs with lidocaine, TEM was performed. **Fig. 5A** shows the TEM images of 2 mM AgNPs having particles size with an average diameter of 20-30

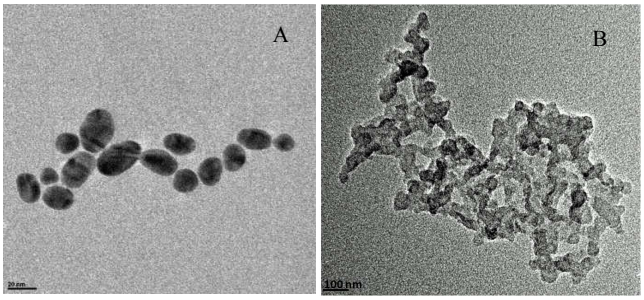

Figure 5A *Size distribution of silver nanoparticle (A) in the presence of lidocaine hydrochloride (B)*

nm and **Fig. 5B** shows the aggregation of AgNPs in the presence of LHC.

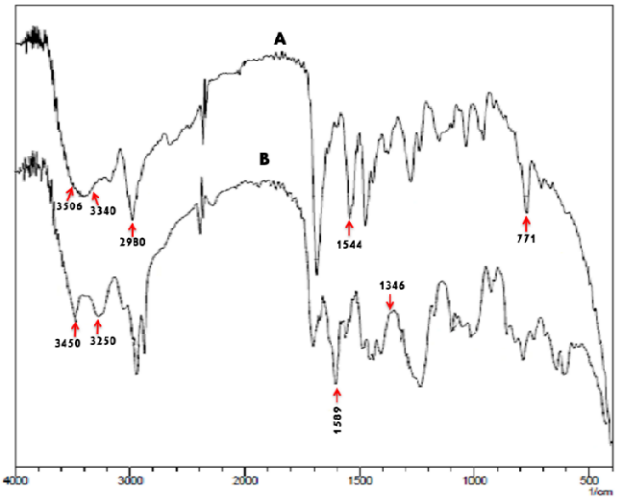

Figure 6 Transmission IR spectra of (A) LHC (B) AgNPs-LHC complex formation

FT-IR analysis

To understand the interactions between AgNPs and lidocaine FT-IR studies were performed. As shown in **Fig. 6**, the results indicated that IR absorption spectra of lidocaine hydrochloride have bands at 3423 cm^{-1}, 3506 cm^{-1}, 3369 cm^{-1}, 3340 cm^{-1} which corresponds to amide N-H vibration, 2980 cm^{-1} (C-H stretch), 1687 cm^{-1} (C=O), 1544 cm^{-1} (amide II) and 771 cm^{-1} (aromatic C-H) as shown in **Fig. 6**. On addition of lidocaine hydrochloride to AgNPs it was found that broadening of amide N-H vibration occurred to 3250 cm^{-1} along with shifting of amide II vibration to 1589 cm^{-1} indicating interaction between the AgNPs and the lidocaine hydrochloride through H-bonding at both the sites. Meanwhile, the appearance of a peak at 3450 cm^{-1} which corresponds to O-H, results in the formation of -C-O-H bond formation indicating hydrogen bonding interaction between the AgNPs and the lidocaine hydrochloride.

ESI-MS

The ESI mass spectrum of synthesised silver nanoparticle was recorded as shown in **Fig**. **S5A**, **see ESI,** which showed a molecular ion peak m/z at 429 and upon addition of lidocaine it showed 701 as shown in **Fig. S5B**, **see ESI,** which provide evidence of the binding of AgNPs with lidocaine.

Optimization of the experimental variables

The influence of the assay conditions including media pH and incubation time was investigated. In order to investigate the optimal pH for effective colorimetric sensing of LHC with citrate-capped AgNPs, UV-visible absorption spectra was carried out in buffer at various pH range from 1.0 to 13.0. The pH of the AgNPs was adjusted by using the PBS buffer. Studies have shown that agglomeration of NPs surfaces at low pH=<4.0 due to neutralization of surface charges will results in changes in their SPR band[39]. Hence lower pH is not recommended for any sensor based investigation. Similar results were also observed in present study as there is colour change from yellow to red indicating agglomeration of AgNPs without addition of analyte (LHC) in low pH range from 1.0 - 4.0, whereas no any change was observed in SPR intensity in pH range from 5.0 – 10.0 as show in **Fig. S6**, **see ESI**. From these results it can be intruded that pH 5.0-10.0 is the suitable pH range for analysis purpose. In the present study pH 7 was selected as optimal pH for further analysis. Since, amino groups of LHC bear positive charge having pKa = 8 (7.86) and citrate molecules on surfaces of AgNPs exhibit negative charges with pKa = <5, yielding strong electrostatic interactions between surfaces of AgNPs and LHC allow AgNPs aggregation. Thus change in SPR band occurs from 420 nm to 506 nm with color change from yellow to red.

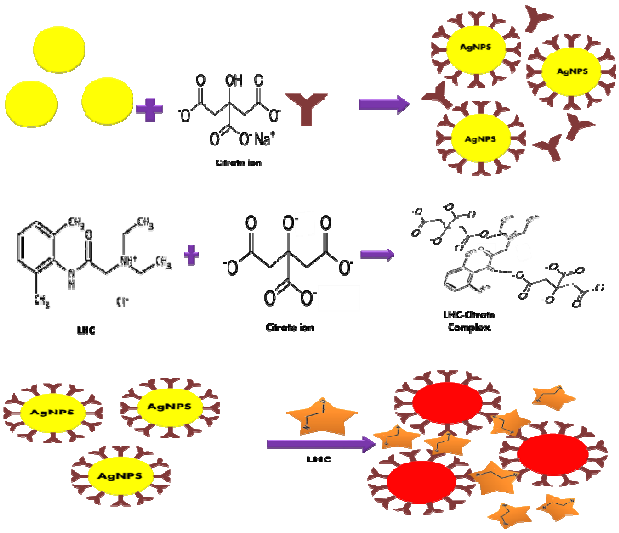

Figure 7 Showing proposed mechanism of lidocaine interaction with silver nanoparticle.

LHC binding mechanism:

It is well known that citrate contains carboxy (-COO-) group which may interact with LHC through H-bonding as crosslink agent and causing aggregation of AgNPs. Consequently red shift is observed in spectrophotometric experiments of citrate capped AgNPs on addition of LHC. Electrons on the alcoholic oxygen get simply delocalized, making it acidic due to easy removal of proton (H^+). The amide group shows basic nature due to presence of lone pair of electron on nitrogen, will contribute in the formation of colored complex between amide of drug and citrate ion of AgNPs. The citrate ions adsorbed on the surface of AgNPs will stabilize citrate-AgNPs in a dispersed state. Citrate stabilized AgNPs were easily aggregated upon addition of LHC via H-bond formation between NH^+ and –COO– groups of citrate ion and between amide group of LHC and –COO– groups of citrate ion, resulting in color change from yellow to red that is used as a simple and selective method for determination of LHC (**Fig. 7**) which is also confirmed by the FTIR study (**Fig. 6**) and ESI-MS (**Fig**. **S5A**, **see ESI**).

Selectivity of the assay

As mentioned earlier, the results ominously indicate that synthesised silver nanoparticles will bind with lidocaine through electro static interaction and hydrogen bonding. To evaluate the high selectivity of the colorimetric assay for lidocaine, other analytes such as acetaminophen, diazepam,

nitrazepam, lorazepam, ambien, atropine and bupivacaine were examined under identical conditions, as shown in **Fig. 8**.

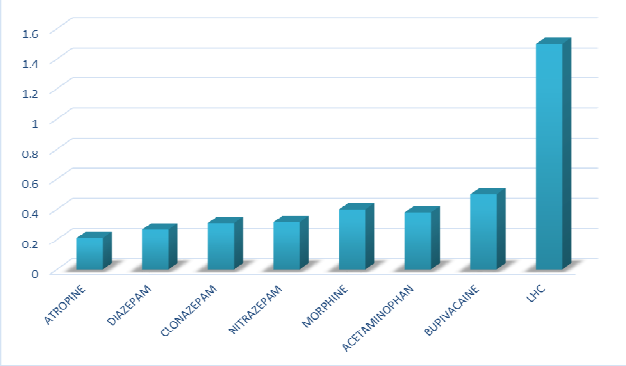

Figure 8 Relative absorbance change of AgNPs at 506 nm in the presence of LHC, acetaminophen, diazepam, nitrazepam, lorazepam, ambien, atropine and bupivacaine.

The above mentioned analytes were opted for selectivity due to either their similar structures or same mode of action. Only after the addition of lidocaine the AgNPs showed color change and the changes in the absorption spectra. It was clear that only lidocaine showed a significantly higher absorbance ratio (A_{506}/A_{420}) compared to other analytes indicating that only lidocaine induces the aggregations of unmodified AgNPs. Further to study the interference of VH, UV-Vis study of VH-AgNPs in buffer medium (pH 7) without LHC was done which showed a peak at 450 nm and concludes no interference in the detection of LHC. Thus the results indicated that unmodified AgNPs represented an excellent colorimetric probe for simultaneous detection of lidocaine.

Sensitivity of the assay

A linear correlation was obtained between the absorption ratio A_{506}/A_{420} and the concentration of LHC in the 0.1 to 4.5 ng/ml range (**Fig. S3, see ESI**). Regression analysis showed a good correlation in the concentration range defined in **Table 1** with 0.12 ng/ml LOQ and 0.05 ng/ml LOD. Whereas by applying the smartphone analysis it was found that image processing by in-built app shows good correlation coefficient as compared to image processing outside the mobile. Use of in-built app may prove more significant in determination of LHC within the linear range but on the other hand UV-Vis spectrophotometer shows more sensitivity with 0.05 ng/ml than in built app which is 0.08 ng/ml.

Method	Linear range (ng/ml)	Regression equation	Correlation coefficient (R^2)	LOQ (ng/ml)	LOD (ng/ml)
UV-Vis Spectrophotometery	0.125-1.25	y = 0.0149x + 0.0688	0.9958	0.12	0.05
Image processing out side the smartphone	0.125-1.25	y = -12.022x + 281.08	0.9939	0.12	0.08
Image processing by in-built App	0.125-1.25	y = -4.1006x + 94.622	0.9972	0.12	0.08

Table 1 Showing LOQ and LOD from the present method

Real sample analysis

In order to validate the applicability of the proposed probe commercial medicinal sample containing LHC, blood and vitreous humor (VH) samples were analyzed. Pharmaceutical dosages were checked to determine whether excipients present in the dosage form interfere with the analysis or not. Moreover, blood and VH were checked to determine the real sample applicability of the proposed sensor. The accuracy of the proposed methods was evaluated by recovery tests after addition of pure drug to the pre-analyzed pharmaceutical dosage of LHC, Blood and VH samples. The drug was then extracted from treated blood and vitreous humor samples by using liquid-liquid extraction method[40]. In brief, blood and vitreous humor samples were diluted first by using 0.5 ml of normal saline and mixed properly. Into this mixture 0.6 ml 1 N of sodium carbonate solution was added to make medium of the solution alkaline which was followed by the addition of 5 ml diethyl ether. After gentle mixing for 5 min, the mixture was centrifuged at 3000 rpm for 10 min and refrigerated at -20^{0}C for freezing. After the mixture was frozen the upper ether layer was collected in clean test tube which was then allowed to evaporate to dryness at 70^{0}C. The residue thus obtained was then dissolved in 0.5 ml of water: methanol (8:2) and was used for further analysis. The extracted samples were first diluted in order to bring it into the linear rage of present method and to obtain quantitative retrieval of the samples. After the analysis with UV-Vis spectrophotometer, Adobe Photoshop CS6 and smartphone app the recovery results obtained were within the range of 98.6% to 103.8% as shown in **Table S1, See ESI**, thus indicating that there are no significant interferences while detecting lidocaine from blood and vitreous humor samples. The results show that the drug mediated aggregation of AgNPs promises great applicability of detecting lidocaine from blood and vitreous humor samples which can prove to be useful in any kind of forensic investigations.

The proposed method for LHC detection was compared with the other techniques it was observed that the present method is highly sensitive and selective than other methods as shown in **Table 2**. Also the detection limit is found to be lowest (0.05 ng/ml) as compared to other reported methods[41-45].

Sr. No.	Method	Detection Limit	Reference
1.	HPLC	1 ng/ml	41
2.	Capillary electrophoresis	3.0 × 10−8 mol L^{-1}	42
3.	Gas chromatography	2.5 ng/ml	43
4.	Capillary electrophoresis	1.8 µg mL^{-1}	44
5.	Hcys-AgNPs	4.6 nM	21
6.	Capillary electrophoresis	2 ng/ml	45
7.	Present method	0.05 ng/ml	--

Table 2 Comparison of the present with other reported work on detection of LHC

Conclusion

In this work, for the first time a novel colorimetric probe is developed for the detection of lidocaine from vitreous humor by using citrated capped silver nanoparticles. The proposed method is simple, rapid, highly selective, highly sensitive and efficient method for lidocaine detection using citrated capped silver nanoparticles probe as the aggregation of AgNPs occurs rapidly in the presence of lidocaine due to the electro-static and hydrogen- bonding interaction between them which results in color change from yellow to red. The method showed good linear correlation in the range from 0.1 to 4.5 ng/ml with a correlation coefficient of 0.9914. The detection limit was found to be 0.05 ng/ml using UV-Vis spectrophotometer, which is much lower than other existing methods. The applicability of the method was checked in real samples of blood and vitreous humor and the results showed high recovery within the range of 98.6% to 103.8%, which proved that the present method have great practical potential for analysis of LHC. Also, the color change from yellow to red can be visually examined and the concentration of the drug can be determined by the use simple application available in free from any smart phone app store. And use of smartphone as image capturing and processing device provides the portability for on spot detection of LHC. The proposed method may prove to be gold standard in forensic toxicology and a novel approach applied for the first time possessing attractive features as it is simple and has on spot detection potential for LHC by the use of smart phone. In future, such procedures will positively help to unravel many analytical and time-consuming problems occurring in clinical and forensic toxicology which eventually can prove to be useful in determination of cause or manner of death.

Acknowledgements

It would not have been possible to perform the study without the financial support of Maulana Azad National Fellowship for minority students, University Grant Commission, India.

References

1. D. Favretto, J.P. Pascali, F. Tagliaro, *J. Chromatogr A*., 2013, **1287**, 84-95.
2. K. A. Rees, N. S. Jones, P. A. McLaughlin, S. Seulin, V. Leyton, M. Yonamine, M. D. Osselton, *Forensic Sci. Int*., 2012, **217**, 182-188.
3. P. Paranitharan and M. S. Pollanen, *Sri Lanka Journal of Forensic Medicine, Science & Law*, 2011, **2**, 22-24.
4. A. J. Jenkins, Drug Testing in Alternate Biological Specimens, Human Press, 2008.
5. P. Fernandez, S. Seoane, C. Vazquez, A. M. Bermejo, A. M. Carro, R. A. Lorenzo, *Anal. Bioanal. Chem*., 2011, **401**, 2177-2186.
6. D. Cox, R. A. Jufer Phipps, B. Levine, A. Jacobs, D. Fowler, *J. Anal. Toxicol*, 2007, **31**, 537-539.
7. L. R. Sanches, S. C. Seulin, V. Leyton, B. A. P. Bismara Paranhos, C. A. Pasqualucci, D. R. Munoz, M. D. Osselton, M. Yonamine, *J. Anal. Toxicol*., 2012, **36**, 162-170.
8. S. Mackey-Bojack, J. Kloss, F. Apple, *J. Anal. Toxicol*., 2000, **24**, 59-65.
9. W. C. Duer, D. J. Spitz, S. McFarland, *J. Forensic Sci*., 2006, **51**,421-425.
10. P. Fernandez, M. Aldonza, A. Bouzas, M. Lema, A. M. Bermejo, M. J. Tabernero, *J. Appl. Toxicol*., 2006, **26**, 253-257.
11. H. M. Antonides, E. R. Kiely, L. J. Marinetti, *J. Anal. Toxicol*., 2007, **31**, 469-476.
12. K. M. Clauwaert, J. F. Van Bocxlaer, E. A. De Letter, S. Van Calenbergh, W. E. Lambert, A. P. De Leenheer, *Clin. Chem*., 2000, **46**, 1968–1977.
13. E. A. De Letter, P. De Paepe, K. M. Clauwaert, F. M. Belpaire, W. E. Lambert, J. F. Van Bocxlaer, M. H. Piette., *Int. J. Legal Med*., 2000, **114**, 29–35.
14. K. S. Scott, J. S. Oliver, *J. Forensic Sci.*, 2001, **46**, 694-697.
15. H. M. Teixeira, F. Reis, P. Proença, P. Ramos, O. Quintela, M. Lopez-Rivadulla, E. Marques, D.N. Vieira, *Hum. Exp. Toxicol.*, 2004, **23**, 571–577.
16. D. Favretto, G. Frison, S. Maietti, S. D. Ferrara, *Int. J. Legal Med*., 2007, **121**, 259-265.
17. A.J. Jenkins, J. Oblock, *Leg. Med*., 2008, **10**, 201–203.
18. H. M. Teixeira, F. Reis, P. Proenc, P. Ramos, O. Quintela, M. Lopez-Rivadulla, E. Marques, D. N. Vieira, *Human & Experimental Toxicology*, 2004, **23**, 571-/577.
19. A. Pelander, J. Ristimaa, I. Ojanpera, *Journal of Analytical Toxicology*, 2010, **34**, 312-318.
20. M. K. Halbert, R. P. Baldwin, *Journal of Chromatography*, 1984, **306**, 269-277.
21. Y. Dou, X. Yang, Z. Liu, S. Zhu, *Colloids and Surfaces A: Physicochem. Eng. Aspects*, 2013, 423, 20-26.
22. *W. Zhiwen, Z. Heping, Y. Keming, Y. Wang, Rom J Leg Med, 2011, **19**, 51-54.*
23. S. K. Lee, S. Y. Lee, S. W. In, H. K. Choi, M. A. Lim, K. H. Chung, H. S. Chung. *Arch Pharm Res*, 2003, **26**, 317-320.
24. R. C Baselt, Disposition of Toxic Drugs and Chemicals in Man, Chemical Toxicology Institute, Foster city, CA, 5th Ed., 2000, pp. 471.
25. D. A. Engelhart, E. S. Lavins, C. B. Hazenstab, C. A. Sutheimer, *J. Anal Toxicol,* 1998, **22**, 246-247.
26. Y. Hino, H. Inoue, K. Kudo, N. Nishida, N. Ikeda, *Forensic. Sci. Int.,* 2001, **124**, 130-136.
27. K. Sakata, S. Ishigaki, M. Sakata, *Forensic. Sci. Int.,* 1988, **37**, 1-10.
28. K. Shimizu, H. Shiono, K. MatsubaraAwaya, T., T. Takahashi, O. Saito, K. Ogawa, H. Mizukami, T. Uezono, H. Akutsu, *Legal Med.,* 2000, **2**, 101-105.
29. Y. Ju-Nam, J. R. Lead, *Sci. Total Environ*. 2008, **400**, 396-414.
30. A. Desireddy, B. E. Conn, J. Guo, B. Yoon, R. N. Barnett, B.M. Monahan, K. Kirschbaum, W. P. Griffith, R. L. Whetten, U. Landman, T. P. Bigioni, *Nature*, 2013, **501**, 399-402.
31. Y. A. Krutyakov, A. A. Kudrynskiy, A. Y. Olenin, G. V. Lisichkin, *Russ. Chem. Rev.*, 2008, **77,** 233-257.
32. A. Lodha, A. Pandya, P. G. Sutariya, S. K. Menon, *RSC Adv*., 2014, **4**, 50443-50448.
33. A. Lodha, A. Pandya, P. G. Sutariya, S. K. Menon, *Analyst*, 2013, **138**, 5411-5416.
34. G. H. Chen, W. Y. Chen, Y. C. Yen, C. W. Wang, H. T. Chang, C. F. Chen, *Anal. Chem*., 2014, **86**, 6843-6849.
35. S. Sumriddetchkajorn, K. Chaitavon, Y. Intaravanne, *Sensors and Actuators B*, 2014, **191**, 561–566.

36. N. Moonrungsee, S.Pencharee, J. Jakmunee, *Talanta*, 2015, **136**, 204-209.
37. L. Shen, J. A. Hagen, I. Papautsky, *Lab Chip*, 2012, **12**, 4240-4243.
38. S. K. Menon, N. R. Modi, A. Pandya, A. Lodha, *RSC Adv*., 2013, **3**, 10623-10627.
39. S. Basu, S. K. Ghosh, S. Kundu, S. Panigrahi, S. Praharaj, S. Pande, S. Jana, T. Pal, *J Colloid Interface Sci*., 2007, **313**, 724-734.
40. G. A. Edhorn, *Canad. Anaesth. Society J*., 1971, **18**, 189-198.
41. A. Sintov, R. Siden, R. J. Levy, *Journal of Chromatography*, 1989, **496**, 335-344.
42. X. B. Yin, J. Kang, L. Fang, X. Yang, E. Wang, *Journal of Chromatography A*, 2004, 1055, 223-228.
43. D. R. Abernethy, D. J. Greenblatt, *Journal of Chromatography*., 1982, **232**, 180-185.
44. G. B. Akyil, H. E. Satana Kara, S. Y. Bas, N. Ertas, N. Gunden Goger, *Turk J Chem*, 2014, **38**, 756-764.
45. J. L. Costa, A. R. Morrone, R. R. Resende, A. A. Chasin, M. F. Tavares, *J. Chromatogr. B*, 2014, **945– 946**, 84-91.

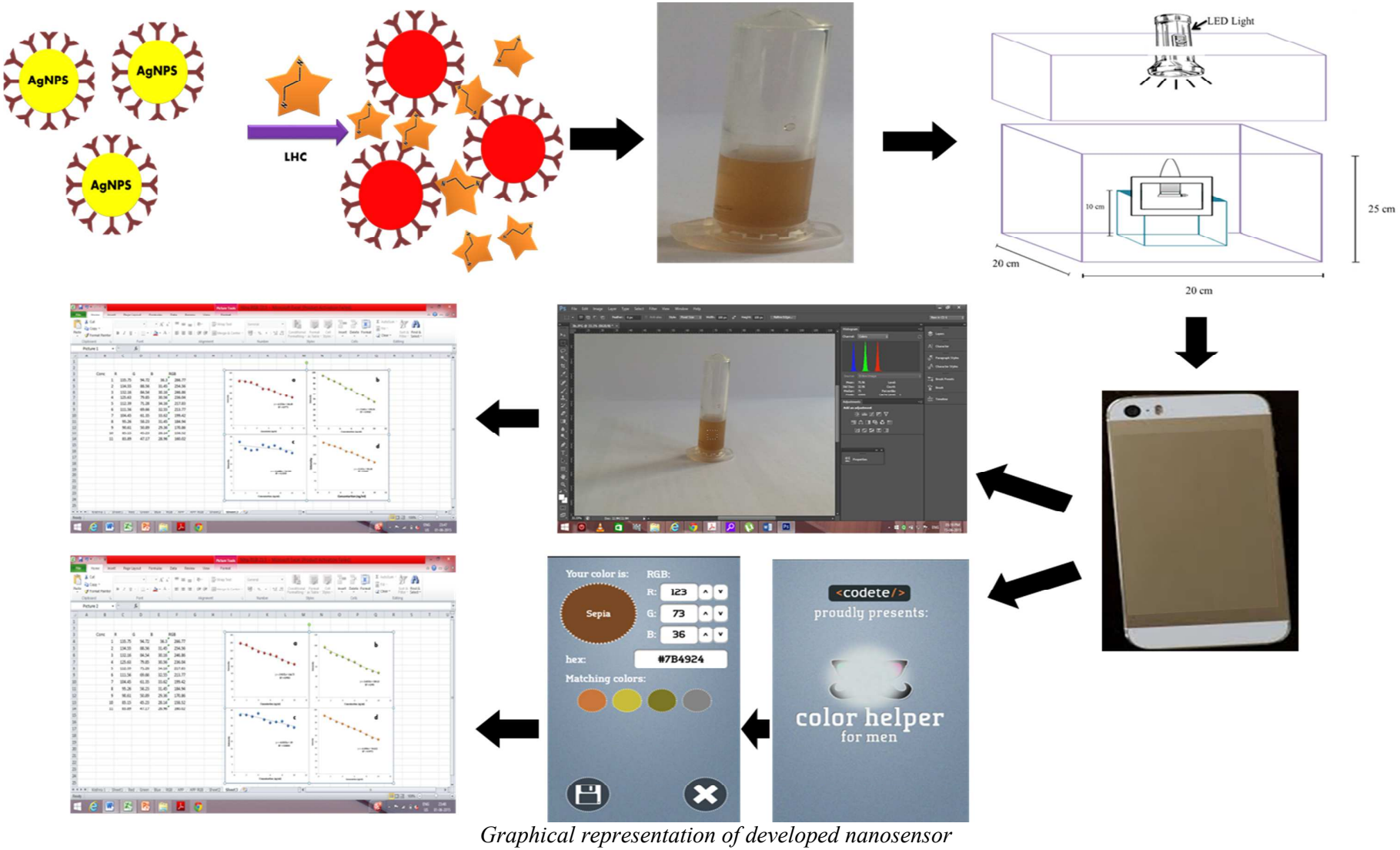

Graphical representation of developed nanosensor